Laboratory experiments on the technical feasibility of the Ocean Battery suction foundation in sand

University of Groningen
Faculty of Science and Engineering
IEM Bachelor Thesis
prof. dr. A. Vakis
dr. ir. A.A. Geertsema

Koen van de Loo
s3161110

January 2020

Abstract

The proposed suction foundation design of the Ocean Battery introduces two elements that are completely novel to the existing technique of suction caisson anchoring;

- A square rather than a cylindrical caisson shape
- Multiple attached suction chambers

The effects of applying these elements on the functioning of a suction foundation are not covered in literature and therefore unknown. Hence, experiments were performed to establish how these design elements influence the behaviour of the foundation and predict the technical feasibility of the design.
It was experimentally found that applying a square caisson shape imposes an increased vulnerability to piping during suction assisted installation, caused by the corners of the shape. Multiple attached suction chambers showed worrying results under self-weight and suction assisted installation. The theoretical self-weight penetration depth of the system was not sufficient for successful suction installation. The validity of the installation tests should be questioned due to scaling issues, but based on these installation tests, the system can't be installed.
If it is possible to install the foundation successfully, the holding capacity of the foundation is not affected by the square shape and configuration. A safety factor of 16 was found together with sufficient resistance to cyclic loading, even in extreme conditions.

Table of contents

Abstract **3**

Table of contents **4**

1 Introduction **5**

2 Problem analysis **6**

2.1 Stakeholder analysis *6*

2.2 System description *7*

2.3 Problem description *8*

2.4 Goal statement *8*

2.5 Research questions *9*

3. Literary research **10**

4. Theoretical background **13**

5. Methods and tools **16**

6. Results **20**

6.1 Installation *20*

6.1.2 Suction assisted installation 21

6.2 Holding capacity *24*

6.3 Cyclic loading *29*

7 Conclusion **30**

8 Discussion **31**

9 References **32**

1 Introduction

A suction anchor, or suction caisson, is a large steel cylindrical structure that is open at the bottom and closed at the top. It is installed into the seafloor by first penetrating under its own weight. After this initial installation step, negative pressure is applied inside the caisson which causes the caisson to force itself into the seabed. This process is show graphically in Figure 1.

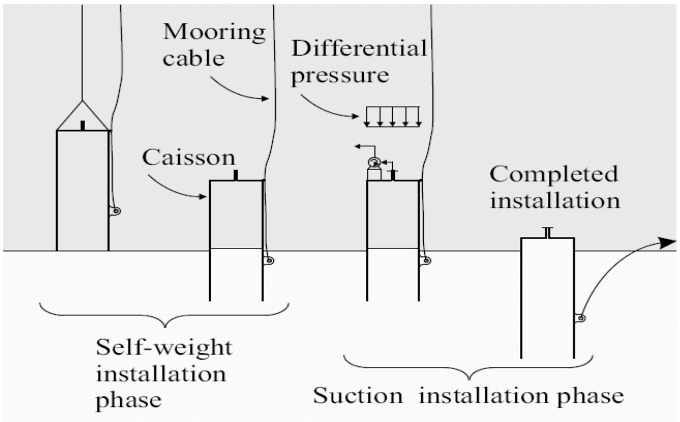

Figure 1 Suction caisson installation [Malhotra, 2011]

Suction anchors have been found to be the most effective anchoring system for floating platforms and offshore structures in deep water (M. Randolph, 2009). Suction foundations offer various advantages over traditional monopile foundations, which are foundations constructed by driving large piles into the seabed.
According to Ukritchon, Wongtoythong and Keawsawasvong (2018), when the installation is successful, the suction developed inside the caisson is maintained, which provides resistance to large uplift as well as lateral loads generated from hydrodynamic (wave and current) loadings acting on offshore structures. Another reason that suction anchors are now commonly applied is that, when technically feasible, they are often cheaper than pile foundations and their installation environmentally friendlier (Van Dijk, 2018). Additionally, suction caissons can be extracted by applying overpressure (Zhang, 2017). This allows for cheaper maintenance and the possibility to relocate the foundation. An example is SPT offshore (2017) that relocated three platforms in the North Sea successfully.

The Ocean Grazer is a Groningen-based company that is working on novel offshore renewable energy solutions and intends to utilize the advantages of suction foundations. Their most recent concept, the Ocean Battery, can store wave and wind energy on-site and provides control over the energy output in every weather condition (Ocean Grazer, 2019). This energy storage system is intended to operate at depths of over 50 meters and needs to be fixed to the seabed. The current design proposes a set of 8 suction anchors, however, for cost saving and design considerations, Ocean Grazer wishes to apply square rather than round caissons as square caissons should be cheaper to produce and fit the square design of the energy storage better. Additionally, these 8 caissons will be directly attached to each other in a square configuration, forming one large suction foundation consisting of multiple suction chambers.

The introduction of a square geometry and the linked configuration are highly unconventional. Research, experiments and case studies on implemented caissons over the past few decades only cover conventional single cylindrical caissons. Consequently, it is not possible to validate the proposed design or predict its behaviour based on literature. Therefore, gathering data on the behaviour of the proposed structure is the essential first step in order to allow for validation and optimization. Empirical data will be collected in lab-scale experiments that can be used to predict the behaviour of the foundation.

2 Problem analysis

2.1 Stakeholder analysis

In order to define the system of interest and scope a stakeholder analysis is performed that identifies the requirements of the problem owner and other stakeholders.
The problem owner in this report is Wout Prins, the inventor of the Ocean Battery and the co-owner of the Ocean Grazer company. He requires exploration into the behaviour and performance of square suction caissons as this is part of his design concept. In order for his company to be successful, the concept needs to be realized. In order for realization, it is essential that the concept is both technically and financially feasible. The possible implementation of square suction caissons could be in important development in the realization process of the Ocean Battery. Hence, understanding the behaviour and performance of a square caisson are of great interest to mister Prins.
Marijn van Rooij is Co-founder and CTO of Ocean Grazer BV. He is invested with the exploration of square caissons too and responsible for supplying equipment and resources to perform lab experiments. It can be concluded therefore that he has significant influence and interest.

The final key player in this research is Antonis Vakis. He is Co-founder and VP of the Ocean Grazer BV and acts as a scientific advisor in the company. As the technical feasibility of Ocean Battery foundation is a scientific problem, this is a topic of concern to him.

Another stakeholder is of this research is R.U.G Houdstermaatschappij B.V (RHM) as they have invested in the Ocean Grazer BV and have an interest in the success of the Ocean Battery. RHM doesn’t have much influence on the outcome of the research, however their interest is significant as the outcome of this research is potentially useful in the further development and success of the ocean grazer. Therefore, consideration should be showed to this stakeholder.

2.2 System description

The structure of the Ocean Battery can be simplified to a housing structure with a concrete reservoir of approximately 20.000 m^3, a square rubber bladder and the foundation. The system utilizes the ocean pressure at large depths to store and release energy by inflating and deflating the bladder. When energy needs to be stored, water from the reservoir is pumped into the bladder that expands into the surrounding higher-pressure water, transforming the electric energy of the pump into potential energy. This energy can be released again by opening valves between the bladder and the reservoir, which causes the ocean pressure to deflate the bladder. As a result of which, the water from the bladder is run through a turbine to recoup the stored energy. Figure 2 shows a cross section of the system and clearly displays the square suction anchors (a) with the concrete reservoir (b) and bladder on top (c).

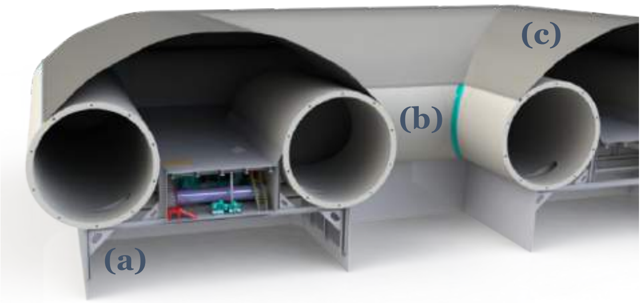

Figure 2 Cross section of the Ocean Battery

The structure measures 60 by 60 meters and weighs almost 34.000 tonnes. The effective weight of the system in water depends on the state of the bladder as the buoyancy force is dependent on the volume of the object/system. When the bladder is deflated, the system has minimal volume and the highest effective weight of almost 8.500 tonnes. In its maximum inflated state, the bladder adds 20.000 m^3 to the volume of the system and due to the increased buoyancy, the effective weight of the system is close to 12.000 tonnes upwards. Therefore, the constant change in buoyancy will subject the foundation to cyclic loading. The frequency of this cyclic loading is unknown at this point as this will depend on the type of usage of the energy storage. Focus of this research is how the suction foundation behaves under the circumstances of the abovementioned Ocean Battery system. The behaviour can be separated into three phases of interest which are also depicted in Figure 3.

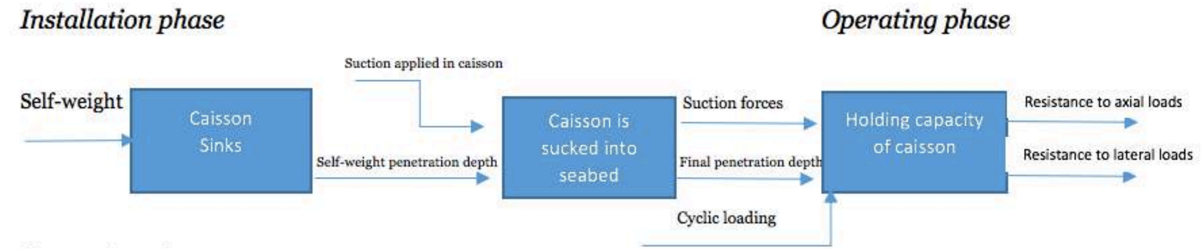

Figure 3 Schematic simplified caisson behaviour

Installation: the foundation has a self-weight penetration depth. This is the equilibrium depth between the buoyancy corrected weight of the system and the frictional forces between the soil and the caisson. Subsequently, negative pressure is created using a pump and a driving force arises that causes the caisson to penetrate further into the seabed. This is called suction assisted installation.

Holding capacity: Once installed, the foundation has a certain resistance to upwards forces. This is called the holding capacity and consists of the friction between the caisson and the soil, the own weight and a suction term.

Cyclic loading: The resistance to cyclic loading is heavily linked to the holding capacity. The foundation experiences stress cycles caused by the inflation and deflation of the bladder that can degrade the holding capacity and cause failure at relatively low upwards forces.

2.3 Problem description

The simplified system described in the system and scope is far more complex in reality. In order to try and grasp all steps of cylindrical caisson behaviour, models have been constructed (Housley, Byrne,2015) (Yeesock Kim) (Alluqmani, 2019) (Anderson 2008) that attempt to predict the behaviour of the caisson during installation and operating. However, developing a robust analytical model that describes the behaviour of suction caisson systems is a challenge owing to, among other factors, the uncertainties in soil characteristics and failure mechanisms postulated. (Yeesock Kim). This problem was also stated by Van Dijk (Van Dijk, 2018), according to him mathematical models were found to be dependent on variables with a high degree of uncertainty. Especially the installation process comes with a degree of complexity as the applied suction pressure and changing depth change the properties of the soil. This can bring about a failure mode called soil liquefaction, which can cause the installation to be stopped (Harireche,2014).

The proposed design of the Ocean Battery introduces two new elements that complicate the modelling even further: the square shape of the caissons and the configuration of fixed caissons. It is of great importance that the foundation design can be validated, however, currently no information is available on the effects of the introducing these elements.

Installing the 8 linked caissons at the same time possibly affects the necessary initial penetration depth or creates a larger sensitivity to unevenness of the soil bed. Additionally, applying suction in caissons directly next to each other possibly limits the flow in the neighbouring caissons. Furthermore, the large amount of waterflow created by applying suction in 8 caissons simultaneously potentially increases the risk of soil liquification. To what extend the holding capacity is affected by neighbouring caissons is not known, but it is expected that there is some degree of interference.

Due to all these uncertainties, information needs to be gathered on whether and how the shape and configuration effect the installation and operating of the foundation. However, as the proposed design is completely novel, no similar foundations have been reviewed in literature. Both the effects of the square shape and configurations on the technical feasibility and behaviour of the foundation are completely unknown at this point

2.4 Goal statement

From the problem statement it becomes clear that new knowledge is necessary in order to make statements on the technical feasibility of the proposed foundation design for the Ocean Battery. The behaviour of the foundation is uncertain due to the introduction of a square shape and configuration. It is unknown whether this introduces problems as no literature or previous research is available. Therefore, the goal is formulated to be:

Experimentally research the behaviour of the proposed suction foundation and determine to what extend it is technically feasible.

With feasibility is meant whether and how the system can be installed successfully and how the foundation copes with upwards forces. This will be tested in the circumstances that will be encountered in the environment of the full-scale system.

The deliverable is a combination of two components:
1) A structured overview of the results, describing the behaviour of the proposed design based on the empirical data generated in the research
2) An educated prediction of the technical feasibility based on the obtained results

2.5 Research questions

The main research question that this research attempts to answer is:

To what extend is the proposed foundation design technically feasible for implementation in the Ocean Battery when installed in sand?

This research question is divided into a number of sub questions that specify the elements of the technical feasibility per process

Installation

- *How is the self-weight penetration depth affected by the shape and configuration?*
- *How do the shape and configuration affect the required initial penetration depth for successful suction assisted installation?*
- *To what extend can the proposed design be installed?*
- *(Is it possible to validate found results with literature?)*

Holding capacity

- *How is the holding capacity affected by the caisson shape and configuration?*
- *Is the expected holding capacity obtained in the experiments sufficient for safely anchoring the system of the Ocean Battery?*
- *How do the empirical holding capacities compare to analytical equations?*

Cyclic loading

- *How does the foundation perform when exposed to the stress cycles caused by the buoyancy of the bladder?*
- *How does the foundation perform when exposed to extreme stress cycles?*

3. Literary research

Offshore anchoring

The first offshore oil rig ‘Superior’ was installed in 1947, 18 miles from the coast of Louisiana in the United States, in just 6 m depth of water. Today, there are over 7,000 offshore platforms around the world located in water depths now starting to exceed 2,000 m (Randolph, 2009). Movement of wind turbines from onshore to offshore (Lynn, 2011) and the development of WECs has caused an increased demand for offshore anchoring techniques for renewable energy sources.

However, offshore anchoring is expensive. The construction costs of offshore wind farms are 1.5–2 times greater than that of onshore wind farms because offshore wind farms require expensive foundations and installation (Oh, 2018). Additionally, the foundation costs are dependent on installation depth. The cost for foundations at the water depth of 40–50m is 1.9 times higher than the cost for the water depth of 10–20 m.

(Randolph, 2009) described the distinguishing features that cause offshore anchoring to be complex and cost intensive.

1. Site investigations are extremely expensive, with mobilisation and hire costs of suitable vessels typically several million US dollars.
2. Soil conditions are often unusual, particularly in respect of carbonate soils and corals.
3. Applied loads are large, with a high component of environmental loading, and large moment loading relative to the weight of the structure.
4. Design modifications during construction are generally not possible or incur severe cost penalties.
5. Emphasis is focused more on capacity, or ultimate limit state, than on deformations although the foundation stiffness is important for the dynamic response of the structure.

The consequences of redesigning the foundation carry large costs, it is of great importance to select the correct anchoring method.

Anchoring methods

A division in anchoring methods can be made between fixed and floating structures, although certain foundations types serve both categories. Fixed structures are directly attached to the embedded foundation, while floating structures are kept in place by mooring cables attached to the foundation.

Gravity-based is the simplest and earliest offshore foundation type, consisting of a heavy cylindrical plate on which structures can be attached, either directly or via mooring cables. This is shown in Figure 4. Gravity foundations are applied for wind turbines in shallow water (0-30 m) (Oh, 2018). They are too heavy and expensive to be installed in deeper waters.

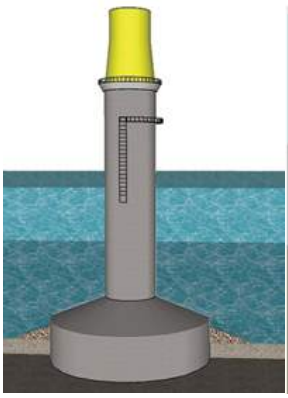

Figure 4 Gravity based foundation (WindTech-international)

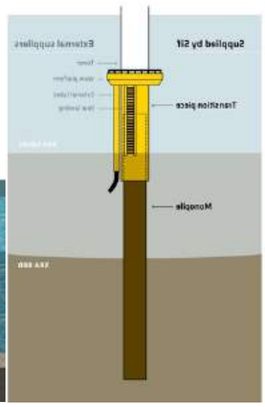

Figure 5 Monopile foundation (IXwind)

However, 91% of European wind turbines in shallow water are anchored by means of monopile foundations (Oh, 2018). This anchoring technique is the most economical for shallow waters in Europe (Rüdiger, 2013) and entails a large pile being driven into the seabed. This process is show in Figure 5. Despite the high holding capacity, this method comes with several drawbacks. The installation is dependent on heavy duty equipment and specialized vessels called jack-up barges. This causes considerable vibration, noise, and suspended sediment. Hence, the installation can cause environmental issues. Ref

Suction anchoring is a more environmentally friendly anchoring technique (Van Dijk, 2018). A suction anchor or suction caisson is a large cylindrical steel structure that is open at the bottom and closed at the top. It is installed by first penetrating the seabed under its own weight after which negative pressure is applied in the caisson to suck it into the seabed.

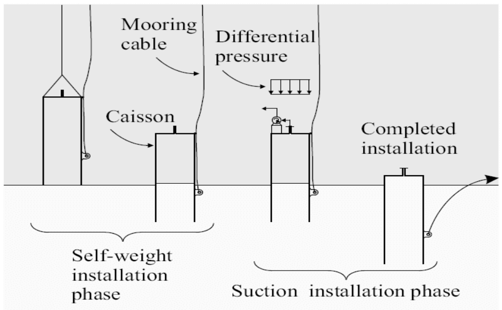

Figure 4 Suction caisson installation [Malhotra, 2011]

Suction anchors have been found to be the most effective anchoring system for floating platforms and offshore structures in deep water (50-200 m) (M. Randolph, 2009). When technically feasible, suction caissons are often cheaper than pile foundations and their installation environmentally friendlier (Van Dijk, 2018). Additionally, suction caissons can be extracted by applying overpressure (Zhang, 2017). This allows for cheaper maintenance and the possibility to relocate the foundation. An example is SPT offshore (2017) that relocated three platforms in the North Sea successfully.

Suction caisson design procedures

Designing a suction foundation is heavily focused on the expected behavior of the foundation. However, this comes with significant complexity due to the complex caisson soil interaction (Yeesock Kim). Multiple approaches have been stated in literature and will be discussed in the following paragraphs. It is important to note that there is no scientific consensus on the nest approach.

Suction caisson laboratory experiments

Multiple experiments with lab scale caissons have been performed to understand how certain parameters influence the behaviour of suction caissons. Additionally, experiments provide empirical data; these can be compared to calculations.

(Hung, 2015), (Sawicki, 2015), (Zhang, 2017) and (Luke,) researched the behaviour during pull out. Responses of the caissons to pull out rates, caisson geometry and extraction manners were examined. Experimental set ups are similar and can be simplified to a reservoir with drained sand, a caisson model, loading system and multiple sensors. (Kou,) and (Zhang, 2017) investigated the installation procedure of the caisson in similar set ups. A schematic overview of lab scale experiments is shown in table 1.

Name	Year	Caisson D (mm)	L/D	Wall thickness (mm)	Material	Type of soil	Reservoir (m)	Type of test	Installation	Pull out rate	Loading system
Yukun Zhang	2017	120	1 2	2 5	Steel Perspex	Chinese sand	1(L) x 1(W)x 0.8(H)	Installation & pull out	Suction	20 mm/s	Pulley block
Nghiem HUNG	2017	150	0.5 1	1	Steel	Silica sand	0.6 (D) x 0.45 (H)	Cyclic loading	Pushing	20 mm/s	Pulley block
Sawicki	2017	100	1	1.5	Steel	Lubiatowo silica sand	0.6 (D) x 0.7 (H)	Pull out	Pushing	20 mm/s	Loading arm
Hai-Lei Kou	2019	120	1	5	Steel	Chinese sand	0,8 (D) x 1 (H)	Installation	Loading rod	-	
A.M Luke	2005	100	0.95	0.81	Aluminium	Clay	1.2(L)x2.4(W)x 1.8(H)	Pull out test	Suction Deadweight	20 mm/s	Winch

Table 1 Overview of suction caisson laboratory experiments

Mathematical modeling of suction caissons

In order to try and grasp all steps of cylindrical caisson behaviour, models have been constructed (Housley, Byrne,2015) (Yeesock Kim) (Alluqmani, 2019) (Anderson 2008) that attempt to predict the behaviour of the caisson during installation and operating.

(Van Dijk, 2018) reviewed numerous available mathematical models and stated that they were dependent on variables with a high degree of uncertainty. Especially the installation process comes with a degree of complexity as the applied suction pressure and changing depth change the properties of the soil.

FEM modeling of suction caissons

Finite Element Method (FEM) was applied in various studies, ranging from installation (Zhou, 2006), holding capacity (Ahn, 2015) to cyclic loading (Zhang, 2017) This method models the soil properties and determines the development of stresses in the soil over depth more accurately than that of mathematical models (Van Dijk, 2018).

Additionally, the stresses in the material of the caisson can also be analyzed to establish whether the caisson design can withstand the forces that are exerted on it and whether the caisson will deform (Cheng, 2016).

4. Theoretical background

The following paragraphs elaborate on the functioning of suction caissons during installation and operating and are intended to provide a better understanding of what factors influence the behavior. A number of accompanying equations is presented, the variables of these are depicted in Table 2.

Table 2 Notation of variables

D_0	Outside diameter	K	coefficient of lateral pressure
D_i	Inside diameter	L	Length of caisson skirt
H_c	Holding capacity	t	Wall thickness skirt
N_q	Overburden bearing capacity factor	γ'	Effective soil unit weight
N_γ	Self-weight bearing capacity factor	δ	Interface friction angle
h	Installed length of skirt	ϕ'	Internal friction angle of soil

System during installation

During installation, the structure is slowly lowered into the water and penetrates the seabed under its own weight. Methods to calculate this self-weight penetration depth are reliant on the penetration resistance of the caisson. This can be modelled by the classical bearing capacity method; however, this brings about some uncertainties. It is dependent on the coefficient of lateral pressure K, which is difficult to measure and has a high degree of uncertainty (Van Dijk, 2018)

The value of K is generally calculated by equation 1 and was proposed by (Das 1986). It is dependent on the internal friction angle of sand, denoted as ϕ'

$$K = 1 - \sin(\phi') \tag{1}$$

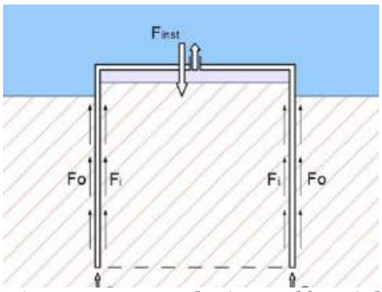

Figure 5 Force during self weight installation [Lembrechts, 2013]

The forces on the caisson during installation are displayed in Figure 4. The self-weight penetration depth is the depth at which the gravitational force of the caisson (F_{inst}) and the frictional forces acting on the skirt tip (Q_{tip}), inside (F_i) and outside (F_o)of the caisson are in equilibrium.

A simplified way of calculating the friction between the caisson and the soil was found by of Houlsby and Byrne (2004) and is shown in Equation 2.

$$V' = \underbrace{\gamma' * \frac{h^2}{2} K\tan\delta_0 \, \pi D_0}_{(a)} + \underbrace{\gamma' * \frac{h^2}{2} K\tan\delta_i \, \pi}_{(b)} \underbrace{(\gamma' h N_q + \gamma' \frac{t}{2} N_\gamma)(\pi D t)}_{(c)} \tag{2}$$

V' is the total friction on the caisson, which consists of three terms. The first term in the equation describes the frictional resistance between the soil and the outer surface of the caisson skirt, the second term describes the friction on the inside. The third term denotes the resistance of the tip of the caisson skirt.

When sufficient initial penetration depth is reached under self-weight, a seal is formed which prevents water from escaping between the soil and the caisson wall when suction is applied. By means of pumping water out of the caisson a driving force is generated down into the seabed. This process is coupled to seepage around the caisson, which produces soil loosening inside the caisson cavity and an overall reduction in soil resistance to caisson penetration (Zhang Y, Li D, Gao Y, 2019). (Houlsby, Byrne, 2015). This process is shown graphically in Figure 5.

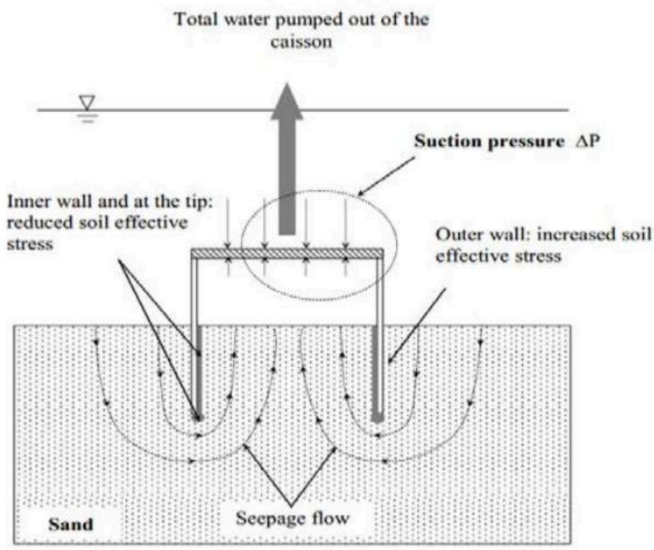

Figure 6 Seepage flow during suction assisted installation (Tran,2005)

This seepage is essential for the installation process (Tran, 2005), but can also cause soil liquification under excessive pressures. This effect originates from replete water flow and causes the soil to lose its strength, hence the installation needs to be stopped. Piping is another undesirable phenomenon that can occur under excessive pressure and involves the formation of channels underneath the skirts of the caisson. These channels cause the seal between the caisson and the soil to break resulting in a failed installation.

System during operation

Once the system is installed into the seabed successfully, the focus is on the maximum force that can be exerted as the vertical pull-out capacity is one of the most important design parameters of suction anchors (Boonchai Ukritchon). The holding capacity consists of the total friction of the caisson, developed suction forces in the caisson and the effective (corrected for buoyancy) weight of the caisson and trapped soil (See Figure 6). However, developing a robust analytical model that describes the capacity of suction caisson systems is a challenge owing to, among other factors, the uncertainties in soil characteristics and failure mechanisms postulated. (Yeesock Kim).

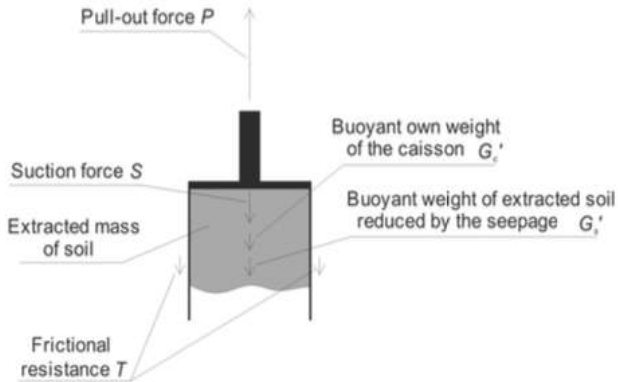

Figure 7 Forces during caisson pull-out [Sawicki, 2017]

A highly simplified formulation of the holding capacity presented by Houlsby Is shown in Equation 4.

$$H_{c} = - U_{SUC} * A(1 + 2L D K \tan \delta) \quad (4)$$

$- U_{SUC}$ is de measured under-pressure under de lid of the caisson and A is the cross-sectional area of the inside of the caisson. $- U_{SUC}$ is taken negatively as the force is caused by a negative pressure. This approach does not incorporate the friction forces separately on the inside and outside as was the case in equation 2.

HUNG described the holding capacity as the sum of the friction on the inside and outside of the skirt with an added suction term. See equation 5.

$$H_{c} = \frac{\gamma' * h}{2} * K * \tan\left(\frac{2\phi}{3}\right) * \Pi * D_{o} * h + \frac{\gamma' * h}{2} * K * \tan\left(\frac{2\phi}{3}\right) * \Pi * D_{o} * h - U_{SUC} * A \qquad (5)$$

This equation is very in line with the situation displayed in Figure 6, however, the buoyant weight of the caisson is not incorporated.

No equations are available that describe the behaviour of suction caissons to cyclic loading, but Hung, Le Chi & Lee, Sihoon & Tran, Nghiem & Kim (2017) found in an experimental study that cyclic loading decreases the holding capacity over time. They found that the holding capacity decreased with the number of load cycles and the load magnitude.

5. Methods and tools

Experiments and testing set ups were designed based on the set ups found in literature and the tools available at the Ocean Grazer lab. The experiments were designed with the specific purpose of answering the research questions.

5.1.1 Caisson models

Tests were performed with 5 caisson models on a 1:100 scale, which were constructed out of metal and Perspex. Initially, tests were only planned with the Perspex models, however, it was found that these had an excessively large wall thickness when compared to the dimensions of the full-scale model. Therefore, two models out of steel were also constructed to provide more realistic results. The models and dimensions can be found in Table 3. From this point the caisson models will be referred to by their coded names.

Table 3 Model caisson specifications

Caisson type	Material	Name	D (mm)	Caisson width (mm)	Caisson length (mm)	Skirt length (mm)	Wall thickness (mm)	L/D	Weight (N)
Single square	Perspex	SSP	/	200	200	110	5	0.55	7.7
Single square	Metal	SSM	/	200	200	110	1	0.55	9.9
Cylindrical	Perspex	CP	200	/	/	110	5	0.55	6.2
Row	Perspex	RP	/	200	600	110	5	0.55	19
Row	Metal	RM	/	200	600	110	1	0.55	21.6

The available set of caissons allows for researching the effect of the square shape and the configuration individually. Using the same skirt length and wall thickness allows for comparing SSP and CP to analyse the effect of the square shape. Similarly, SSM and RM allows for researching the effect of the proposed configuration.
Each caisson is equipped with a valve; this valve can be opened, closed or be attached to a tube from the pressure reservoir. This allows for both suction assisted and manual installation of the caisson. Additionally, each caisson is equipped with evenly spaced screw eyes that connect the caissons to the loading system and sensors. See Figure 10, in which the valves of the SSP and RP model are closed.


Single Square Perplex (SSP)

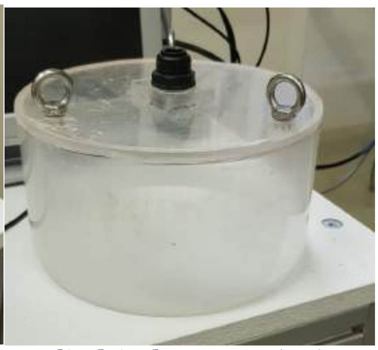
Cylindrical Perspex (CP)


Single Square Metal (SSM)

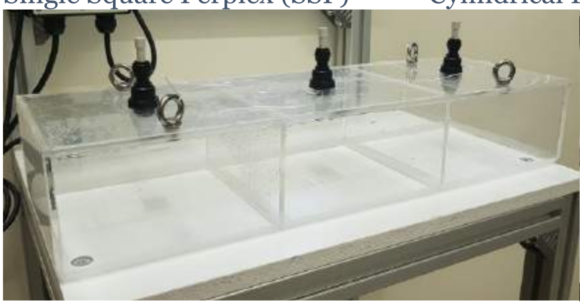
Row Perspex (RP)


Row Metal (RM)

Figure 8 Pictures of model caissons with screw eyes and valves

5.1.2 Soil bed

The soil bed used in this thesis was prepared in a large rectangular fiberglass container measuring 8m in length, 0.8 m in width and a height of 1 m. The sides are made of glass allowing for observations to be made during the experiments. A picture of the container and soil bed is shown in Figure 11. The container was filled with 20 cm of silica sand; which is quartz (SiO_2) broken down into small particles with grain size of 1 mm or less. This type of sand is also used in the experiments of (Sawicki, 2017) and (HUNG, 2017) described earlier.

Figure 9 soil bed

Subsequently, fresh water was pumped into the container forming a water column of 15 cm. The soil bed was left to rest multiple days to ensure full saturation of the sand. The properties of the soil were not measured as this required equipment and expertise that was not available. Hence, the properties were taken from (Sawicki, 2017) and are displayed in Table 4.

Table 4 Properties of silica sand (Sawicki, 2017)

D_{10}	0.15 mm
D_{60}	0.20 mm
Unit weight of sand grains	25.8 kN/m^3
Unit weight of dry sand	15.8 kN/m^3
Unit weight of saturated sand	19.7 kN/m^3
Internal friction angle	34.0 °
Friction angle between soil and model walls	9.7 °
Porosity	39%
Void ratio	0.55
Void ratio	0.82
Coefficient of permeability	1.54×10^{-3} M/S

5.1.3 Testing set up

Multiple aspects of the foundation design were tested. Hence, multiple different set ups were required. The different variations of set ups used throughout this paper will be described below.

Installation

The installation behaviour of the caissons was tested in the sand bed. Directly above this sand bed, a displacement sensor was installed to which the caissons could be attached via metal chains. Multiple weights of 0.5 kg were available to apply static loadings and track the penetration of the caissons under increasing self-weights as shown in Figure 12.

Figure 10 selfweight penetration testing

An electric pump attached to a 250 Litre reservoir was in place next to the container with the sand bed in order to research the suction aided aspect of installation. From this reservoir, tubes could be connected to the caisson in the soil bed allowing suction assisted installation. These tubes were equipped with valves that allowed to control the flow of water and sand being extracted. This set up is schematically drawn alongside pictures of the real set up in Figure 13.

This reservoir serves multiple functions; it can be set to a desired under-pressure to test with and maintains a constant pressure due to the large volume. Additionally, it also stores the water and sand that are extracted during suction installation.

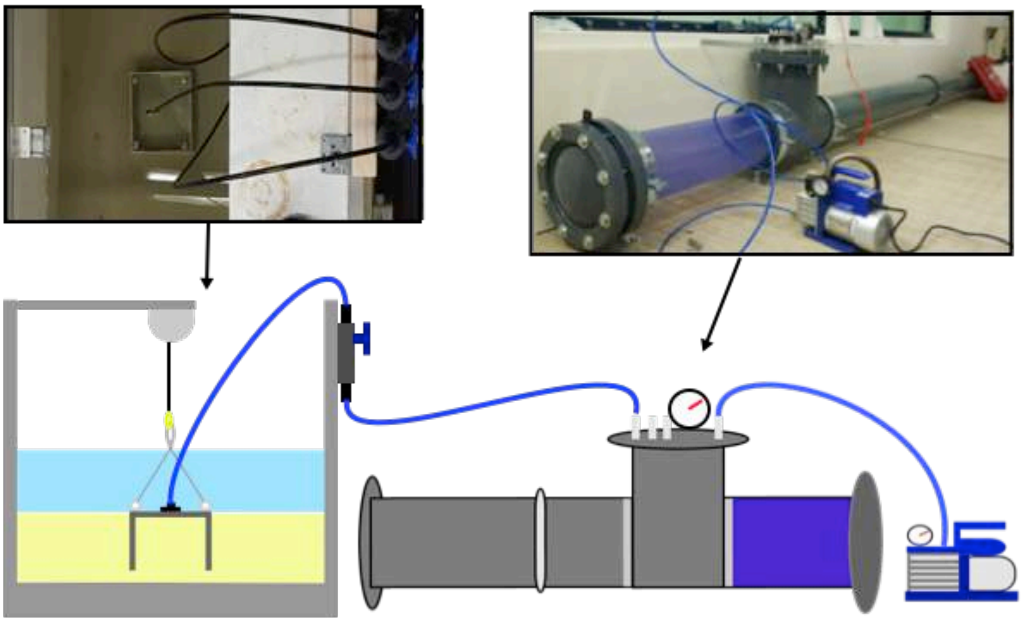

Figure 11 Schematic overview of suction installation set up. The container is depicted from a side view.

Holding capacity

A motor with a lashing strap winding mechanism was installed on top of the container. The rotational frequency of the motor could be set to speeds varying between 11.4 and 60 rotations per minute via a control panel. A steel cable was attached to the lashing strap on the motor axel and was run over a pulley block above the sand bed. Several items were connected to this cable; a weight to keep the cable in place, a force cell with a maximum capacity of 3 KN to measure pull out forces and a calliper clip that allowed to attach the caissons to the cable. The data of both sensors were recorded by the program LabView. The simplified set up is schematically shown alongside pictures of the used set up in Figure 14.

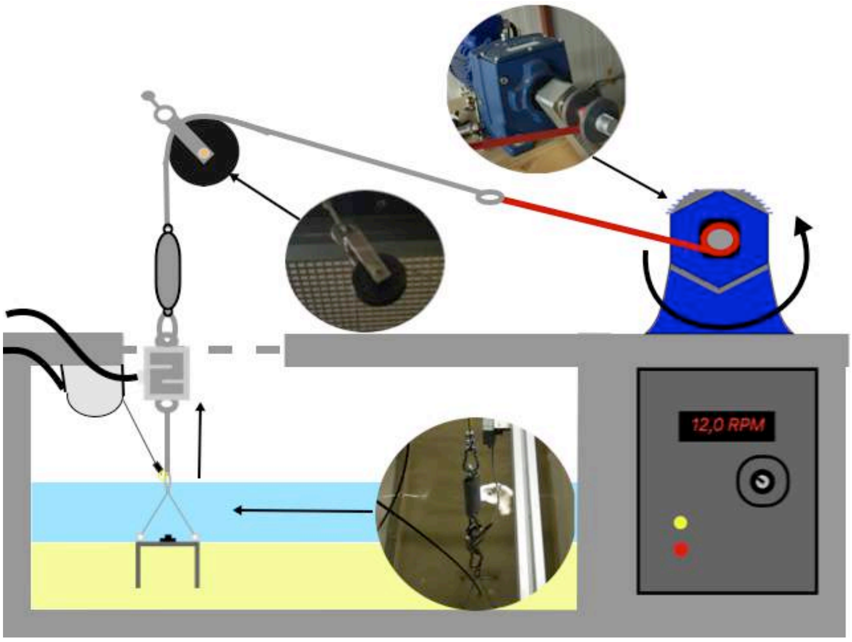

Figure 12 Schematic overview of holding capacity set up alongside pictures of important components. The container is depicted from a front view.

Cyclic loading

The behaviour of the foundation under cyclic loading was tested with a set up very similar to that of testing the holding capacity. It is displayed in Figure 15. The attachment on the motor was changed to an arm with a rotational head to which the cable was connected, creating a cyclic pull on the cable every full rotation of the motor.

The cable from the motor was run over the same pulley block as in the holding capacity set up and springs with a K constant of 1,3 N/cm were used to attach the caissons to the calliper clip hanging from the load cell. The magnitude of the exerted pull could be set by calculating the required expansion of the spring and set the arm of the motor accordingly.

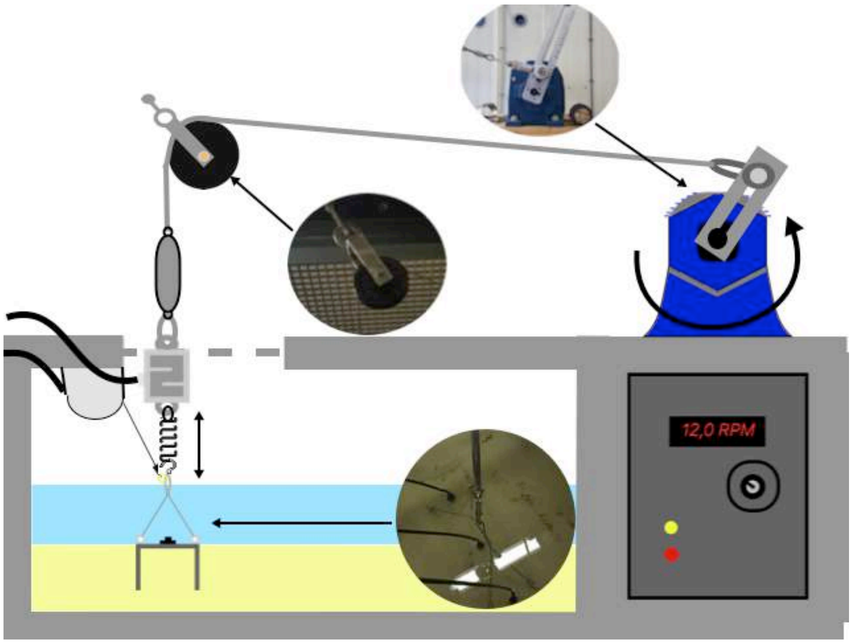

Figure 13 Schematic overview of the cyclic loading test set-up. The set-up is depicted from a front view.

6. Results

6.1 Installation

6.1.1 Self weight penetration

Using Equation (2) of Houslby & Byrnes, the theoretical self-weight penetration depths of the scaled caisson models were calculated.

$$V' = \gamma' * \frac{h^2}{2} (K\tan\delta)_0 \pi D_0 + \gamma' * \frac{h^2}{2} (K\tan\delta)_i \pi D_i + (\gamma' h N_q + \gamma' \frac{t}{2} N_\gamma)(\pi D t) \quad (2)$$

To adjust for the square shape, terms and were replaced by the outer and inner skirt circumference respectively. Resulting in Equation (6)

$$V' = \gamma' * \frac{h^2}{2} (K\tan\delta)_0 C_0 + \gamma' * \frac{h^2}{2} (K\tan\delta)_i C_i + (\gamma' h N_q + \gamma' \frac{t}{2} N_\gamma)(C_i t) \quad (6)$$

Equation (6) was rewritten as a quadratic function in terms of which allowed to solve the penetration depth corresponding to the soil properties and weight and dimensions of the caisson. See Equation (7).

$$h^2 \left(\frac{C_0 + C_i}{2} \right) K\tan\delta + h\left(C_i N_q + \frac{C_i t}{2} N_\gamma \right) - V' \quad (7)$$

In which K was calculated using Equation (1),γ was set at 8 KN/m³, was set at 25 and the corresponding bearing capacity factors and were selected from Mayerhoff to be 10,7 and 6,8 respectively. The results obtained are shown in Table 5.

Table 5 results of theoretical self-weight penetration depths

	Weight (N)	HOULSBY & BYRNE Force for full penetration (N)	Self-weight penetration depth	Percentage of skirt length
SSP	7,73	113,25	0,75	7
SSM	9,90	56,45	1,93	18
CP	6,20	90,86	0,75	7
RP	19,00	321,34	0,65	6
RM	21,60	148,68	1,60	15

Using this method on the specifications of the Ocean Battery results in a theoretical self-weight penetration depth of 2,28 m. This is 20% of the skirt length.

Self -weight penetration depths could not be obtained experimentally. The Perspex caisson models would tip over when placed on the soil bed and resetting the displacement of the sensor when placing the model exactly on the soil bed showed very large deviations and inaccuracies. Hence, the behaviour of the models was analysed in a higher range of mass and displacement. The weights of the models were gradually increased by steps of 5N. The results are shown in Figure 16**.** Initial self-weight penetration depths were set to zero before applying the weights. Each weight was rested for 15 seconds to allow for full displacement under the weight

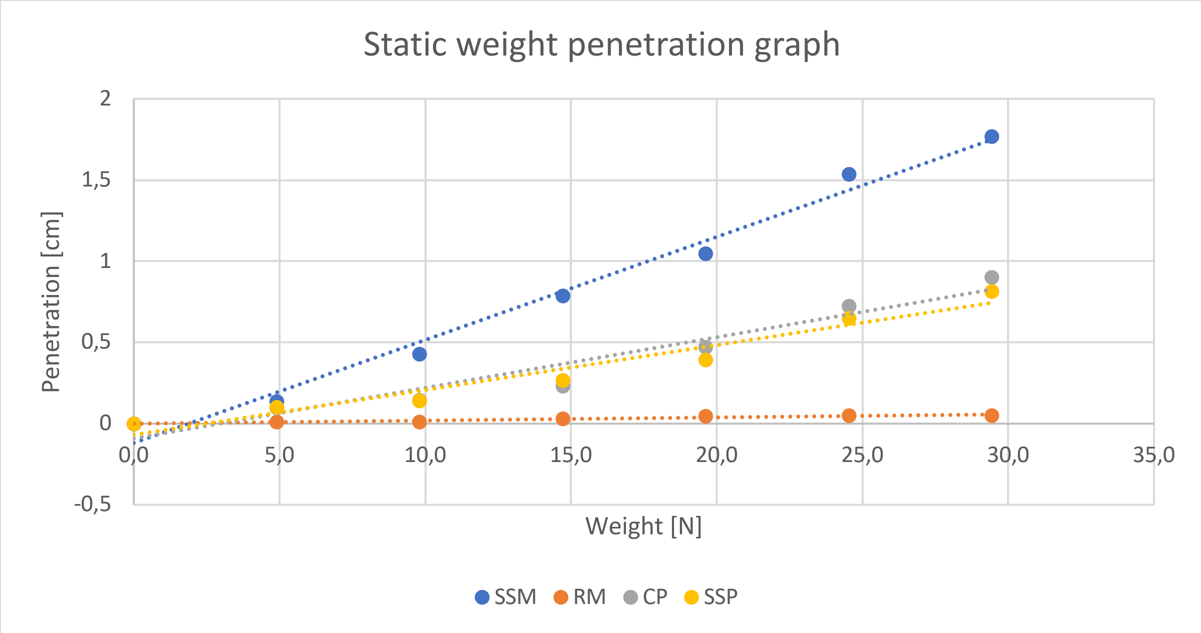

Figure 16 Penetration depths under increasing static weight

The obtained penetration depths are significantly lower than the values obtained in Table 5. A possible explanation for this is the scale of the experiment. The caisson models are scaled 1:100, however the sand is not. Therefore, the sand grains are out of proportion with the caisson dimensions resulting in a more difficult penetration of the soil bed. However, the results are still useful for establishing potential differences in behaviour due to shape and multiple chambers.

Assessing SSP and CP, no noticeable differences are found in the self-weight penetration behaviour of the two caissons. Therefore, it is concluded that the introduction of a square shape does not impose undesirable effects on the self-weight penetration behaviour of the foundation

It was expected that due to the larger frictional area (factor 2.5) of the RM model, its slope would be reduced by at least this factor when compared to the SSM model. However, it was found to perform considerably worse than that with hardly any displacement found. A potential cause is that due to the larger area of the model, it is more vulnerable to unevenness of the soil. As only the displacement of the entire model could be tracked, it is possible that due to soil unevenness the model displaced under an angle.

6.1.2 Suction assisted installation

Suction installation tests were performed under various initial penetration depths to establish possible differences caused by the square shape or multiple caissons. Initially, set under-pressures in the reservoir were used, leading to the formation of piping channels as the pressure was excessively large and applied too quickly. Hence, the installations were performed with no initial under-pressure and the suction was ramped up slowly by the pump, equivalent to how suction installations are carried out in practice. This allowed for successful installations.

However, during certain tests, the caisson would initially displace under the corresponding pressure but form piping channels as this pressure increased. It was found that maintaining a steady under-pressure by switching off the pump for intervals of 20 seconds, decreased the formation of piping channels and allowed caissons to be installed at penetration depths that would lead to piping under ramp suction installation.

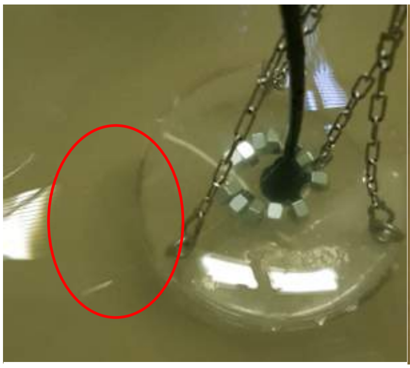

Figure 17 Piping formation arbitrary place CP model

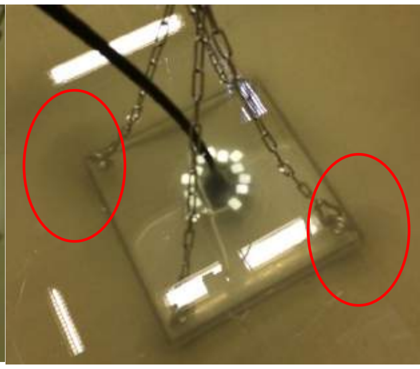

Figure 18 Piping channels at the corners of SSM model

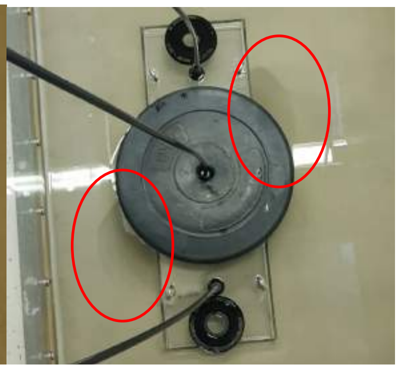

Figure 19 Piping channels at bordering chambers of RP model

The place at which piping channels were formed differed per caisson model. For the CP, representing the traditional caisson, piping channels were formed at an arbitrary place (Figure 17) while for the square caissons (SSM & SSP), piping would occur around the corners of the model as depicted in Figure 18. This specific placement of channels signals that the corners affect the flow during suction installation. For the multiple chamber caissons (RM & RP), piping occurred at the sides of bordering chambers (figure 19), indicating that the suction installation is affected by the introduction of multiple chambers. This interference is stronger than that of the square shape as no channels are formed at the outlying corners.

The results of the suction installation test are shown in Table 6, which indicates for every caisson whether installation was successful at multiples of 10% of the skirt length initially installed.

Table 6 Suction installation results

Penetration depth	6,6 cm	5,5 cm	4,4 cm	3,3 cm	2,2 cm	1,1 cm
Percentage of skirt length	60%	50%	40%	30%	20%	10%
RP	X	X	X	X	X	X
SSP	✓	✓	✓	✓	X	X
CP	✓	✓	✓	✓	✓	✓
SSM	✓	✓	✓	✓	✓	✓
RM	✓	✓	✓	✓	X	X

The symbols in Table 6 can be explained as follows: ✓ indicates a successful ramp suction installation, ✓ denotes successful installation by using suction intervals and X denotes the formation of piping channels.

Single caissons

Comparing the installations of CP and SSP shows that the square caisson shape introduces an increased vulnerability for piping. The material, wall thickness and skirt length of the models are identical, additionally the testing conditions were also kept constant between the tests. Hence, the significantly higher initial penetration depth (30% vs 10%) of the square caisson is due to its shape. Interestingly, this is not a reason for concern for the Ocean Battery. The SSM model measures a realistic wall thickness and requires an initial penetration depth of 10% of its skirt length. From this it is concluded that the wall thickness is a more important geometry factor than the shape for the foundation design of the Ocean Battery.

Multiple linked caissons

It was found that the RP model could not be installed, even when suction intervals and high initial penetration depths were applied. This indicates that multiple chamber caissons have a more complex installation process than singular caissons. Comparing the SSM and RM models is more accurate as they have a realistic wall thickness. Results show that the RM could be installed with an initial penetration depth of 30%. This is problematic for the foundation design as this exceeds the theoretical self-weight penetration depth of the system, suggesting that the proposed design cannot be installed.

The displacement of the RM and SSM models was recorded under the identical initial penetration depth (3,3 cm), ramp suction and flowrate. The graph is displayed in Figure 20.

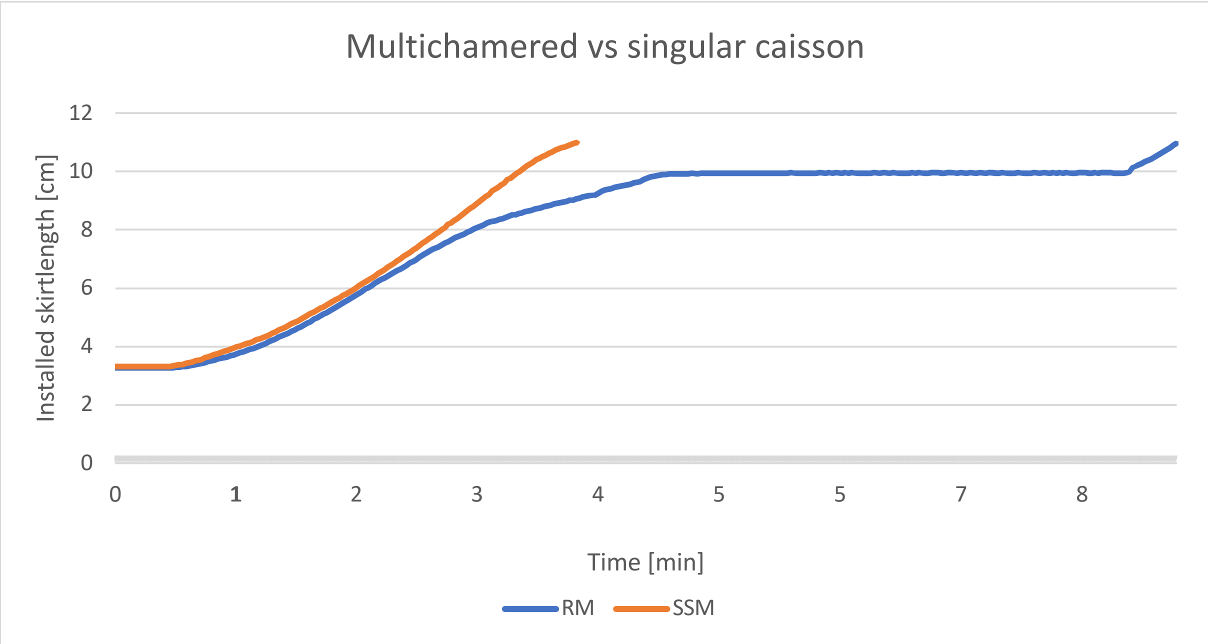

Figure 20 Suction installation of RM and SSM caisson

The initial displacement of both models is almost identical, however after 7 cm of the skirt installed, the displacement of the RM stagnates and stalls at a depth of 10cm. After which no further displacement happens until the flowrate is increased. See the graph, approximately 8 minutes into the installation.

6.2 Holding capacity

6.2.1 Single caissons

Pull out tests were performed with the caissons installed both manually and via suction. The force curves of the single caissons are displayed in Figure 21. The general shape of the force curves does not show any noticeable distinctions between the caissons. The found curve is almost identical to the one presented in Sawicki's paper. The pull outs were performed with identical motor settings, in which the caissons were extracted in approximately 6 seconds.

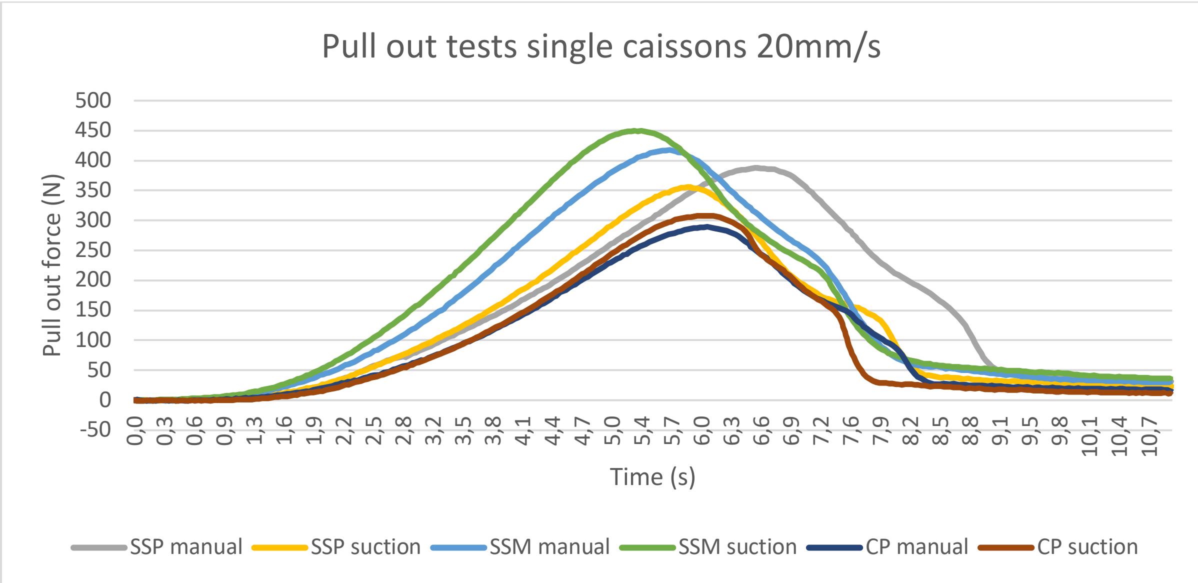

Figure 21 Pull out tests single caissons

Holding capacities were found to vary between 289 N and 451 N. For all caissons, it was found that the holding capacity varied slightly between suction and manual installation with a maximum difference of 8%. Manual installation gave a higher holding capacity for the SSP and SSM models, while suction installation resulted in a higher holding capacity for the CP model.

To investigate the effect of resting time between installation and pull out, resting times were tested between 5 minutes and 12 hours. It was found that this did not affect the holding capacity. Nevertheless, a resting time of 10 min was utilized to provide for consistency between tests.

When analysing the effect of the shape it is found that the square caisson (SSP) gave a higher holding capacity than the round caisson (CP). However, this can be explained by the larger volume and surface area of the square caisson presented in Table 7.

Table 7 Comparison of holding capacities SSP and CP

	Manual HC (N)	Suction HC (N)	Average HC (N)	Frictional area (cm^2)	Volume (cm^3)
SSP	388	356	372	1716	3971
CP	289	309	299	1348	3119
Factor	1,34	1,15	1,24	1,27	1,27

Examining the holding capacity per frictional area and volume shows very similar results for both caisson models. It is concluded that the introduction of a square caisson shape does not evidently impose negative effects on the holding capacity of the caisson

Figure 22 shows the force curve plotted against the displacement of the CP and SSP model.

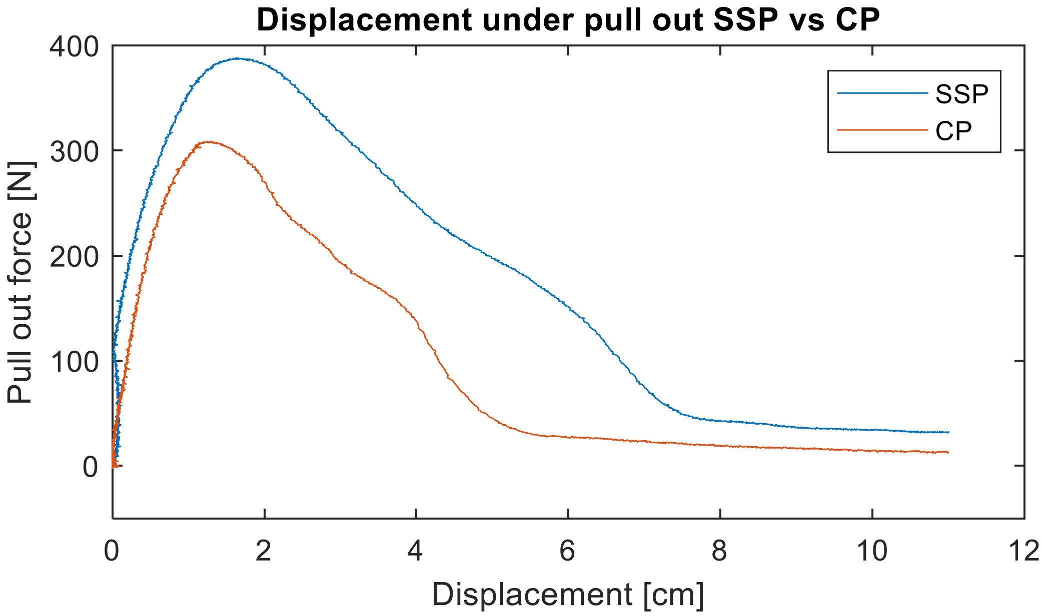

Figure 22 Displacement under pull out SSP vs CP models

Assessing the curves of the SSP and CP further does not show significant differences. The CP model measured its maximum force at a fractionally smaller displacement than the SSP model, but the general shape is almost identical indicating that the behaviour of a square and a cylindrical caisson during pull out is identical.

6.2.2 Multichambered caissons

The force curves under pull out of the RM and RP caissons are displayed in Figure 23. As RP could not be installed successfully via suction only a manually installed pull out test was performed with this caisson.

Holding capacities varied between 1.12 KN and 1.25 KN. Pull outs were performed with the constant resting time of 10 min and identical motor settings resulting in approximately 6 second pull outs.

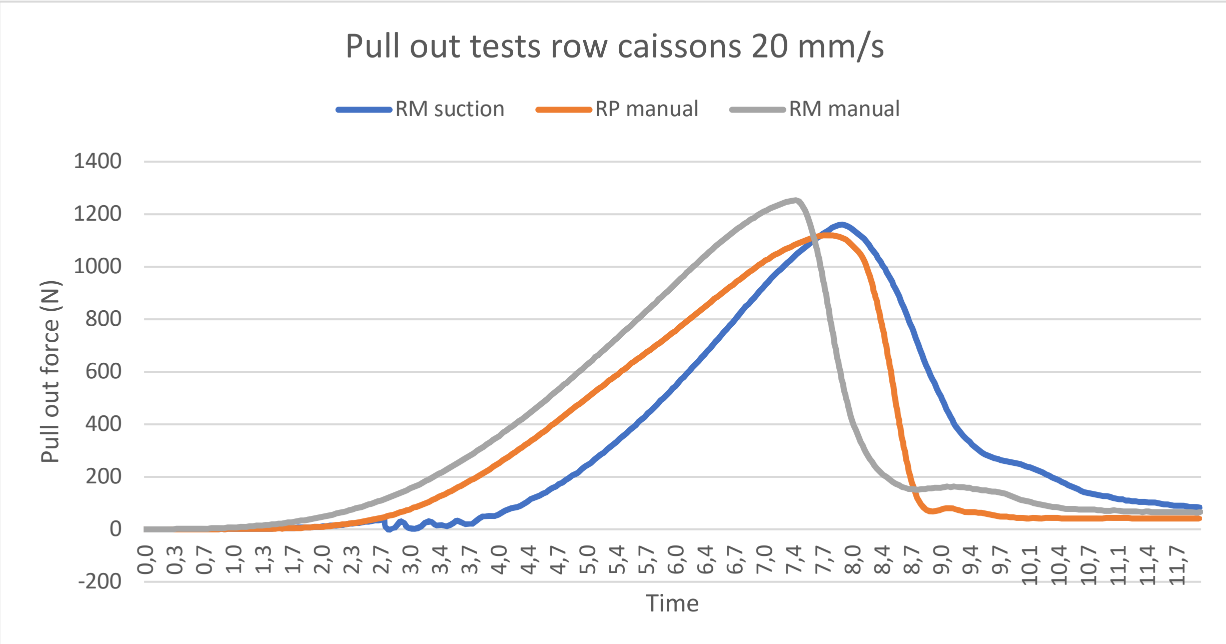

Figure 23 Max pull out forces of multichambered caisson

Suction installation gave an 8% higher holding capacity than manual installation for RM, identical to the results of SSM and SSP. Compared to the force curves of the single caissons, the slope after reaching the maximum pull out force is far steeper for the row caissons. This indicates that the holding capacity degrades (at a higher pace) once the maximum force displacement is reached. This can be explained by observing the caissons under pull out (Figure 24) as the multichambered caissons came out of the soil at a tilted angle.

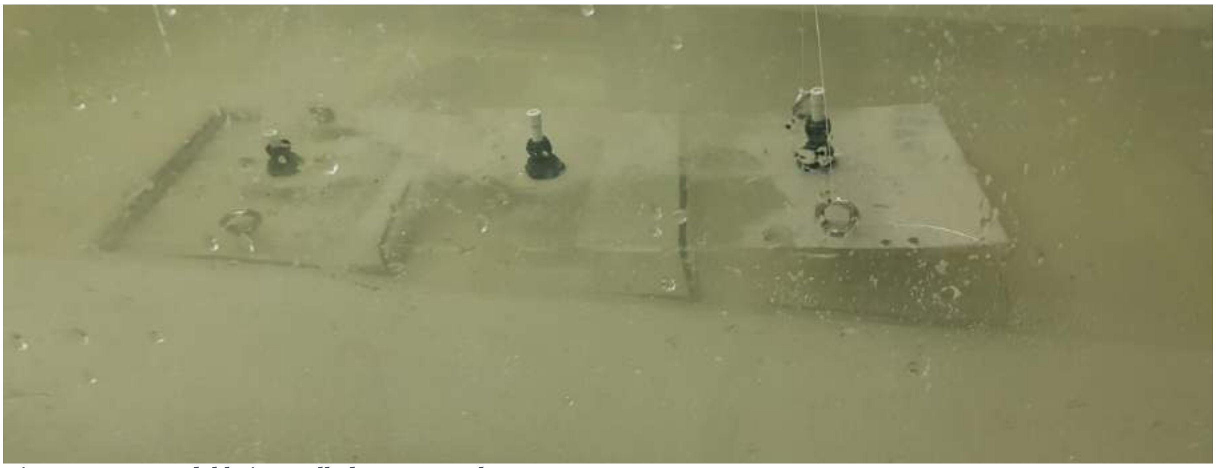

Figure 24 RP model being pulled out an angle

Only the displacement of the caisson as a whole could be tracked during installation rather than each of the three chambers separately. Hence, it is probable that one of the two chambers on the side has a marginally lower installation depth causing it to have a slightly lower holding capacity. As a result, this chamber displaces earlier and once it reaches its maximum force displacement, the holding capacity of the entire caisson degrades at once, causing the steep slope in the diagram.

To analyse the effect of multiple linked suction chambers rather than the conventional singular design, the results of RM and SSM are compared in Table 8.

Table 8 Comparison holding capacities RM and SSM

	Manual HC (N)	Suction HC (N)	Average HC (N)	Frictional area (cm^2)	Volume (cm^3)
RM	1253	1160	1207	4378	12981
SSM	451	418	435	1751	4312
Factor	2.778	2.775	2.777	2.500	3.010

The holding capacity of the RM model was found to be approximately factor 2,8 of that of the SSM model, while essentially consisting of three linked SSM models. The frictional area factor being less than 3 can be explained by the shared walls inside the SSM model. Assuming that both the volume and the area are factors that influence the holding capacity, the effects of linking multiple caissons are negligible. It is concluded that the effects of interference are unsubstantial and therefore linking multiple caissons is not a point of concern for the holding capacity of the Ocean Battery foundation.

Figure 25 shows the force curve plotted against the displacement of the SSM and RM model.

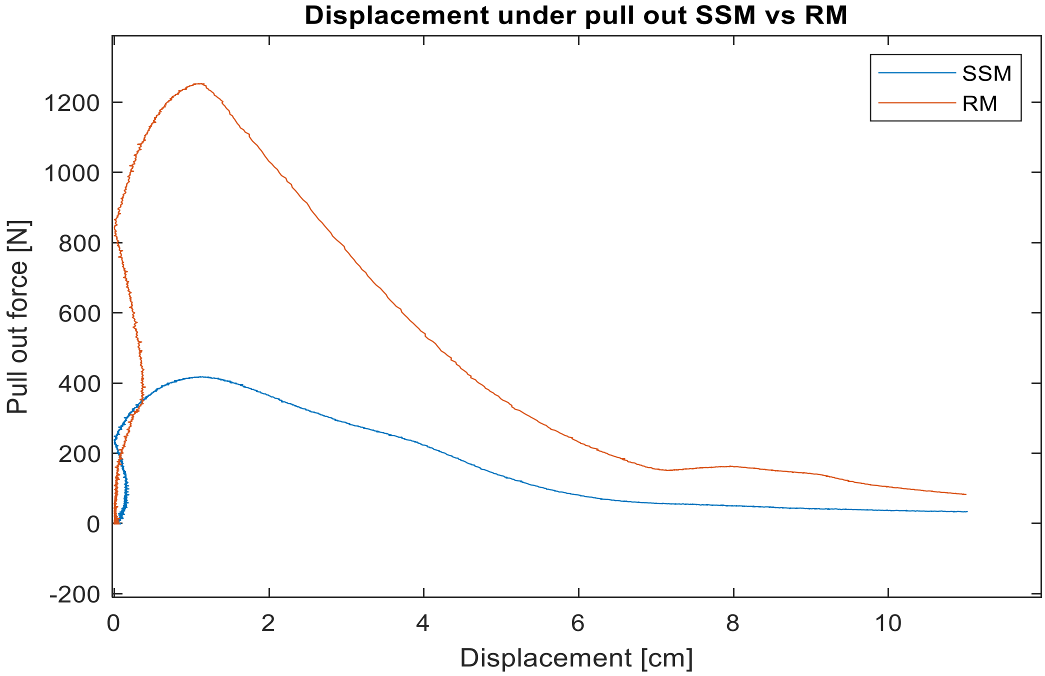

Figure 25 Displacement under pull out SSM vs RM models

Both models measure their maximum force at the same displacement. Additionally, both models show the same general force displacement behaviour, only the slope of the RM model is far steeper after reaching the maximum force. This means that once reaching critical displacement, a set of linked caissons proportionally needs less force for further displacement than a single caisson. This is a point of concern for the Ocean Battery foundation

6.2.3 Results vs calculations

Equations 3 and 4 were used to compute the theoretical holding capacities of the caissons. Due to the absence of a pressure sensor inside the caisson, was taken from literature and set at -6,76Kpa. The internal friction angle was set at 25 and the corresponding bearing capacity factors were selected from Meyerhof (ref). Table 9 displays the calculated and recorded holding capacities and the according displacement at which this was measured.

Table 9 Theoretical vs experimental holding capacities of model caissons

		Theoretical HC (N)		Experiment		
Caisson	**Installation**	**Houlsby**	**HUNG**	**Measured HC (N)**	**Displacement max force (mm)**	**% of skirt length**
CP	Manual	283	254	289	16.34	14.86
	Suction			309	13.14	11.94
SSP	Manual	340	309	388	15.63	14.21
	Suction			356	11.21	10.19
SSM	Manual	369	332	451	12.06	10.97
	Suction			418	11.62	10.57
RM	Manual	1020	926	1253	11.16	10.15
	Suction			1160	13.49	12.26
RP	Manual	1108	926	1120	25.68	23.34

It was found that the holding capacity of each caisson was measured to be higher in the tests than the theoretical values. Furthermore, it should be noted that the accuracy of the square shape and row calculations (82%) was lower than the overall accuracy (85%) and the accuracy of the traditional cylindrical caisson (93%), suggesting that improvements can be made in the equations for square shape holding capacity.

The displacement of the caisson lid at which the maximum force was recorded was on average 13% of the skirt length. This is the identical percentage that was found in the experimental study of (Luke, 2005).

6.3 Cyclic loading

Table 10 displays the results of the cyclic loading tests on the RM caisson. The RM model was used as it includes the square caisson shape, multiple linked chambers and a representative wall thickness. Hence, it is the most realistic test case of the real Ocean Battery foundation.

Table 104 testing condition specifications

	Realistic conditions	Extreme conditions
Frequency	0,2 Hz	0,4 Hz
Magnitude	0-75 N	50-112,5 N
Number of cycles	2700	2700
Max displacement	0,13 cm	0,72 cm

The model was installed via suction and subjected to 2700 stress cycles. Realistic conditions were applied in which the magnitude of the load cycles alternated between 0N and 75N, the scaled force on 3 chambers caused by the inflation and deflation of the rubber bladder. The lowest available testing frequency was 0.2 Hz.
Extreme conditions were also tested in which the system was under tension at all times. Load alternated from 50N to a maximum force of 112,5 N, a safety factor of 1,5 of the realistic conditions and the frequency was doubled to 0.4 Hz.

The results of imposing these conditions on the displacement of the RM model are displayed in Figure 26.

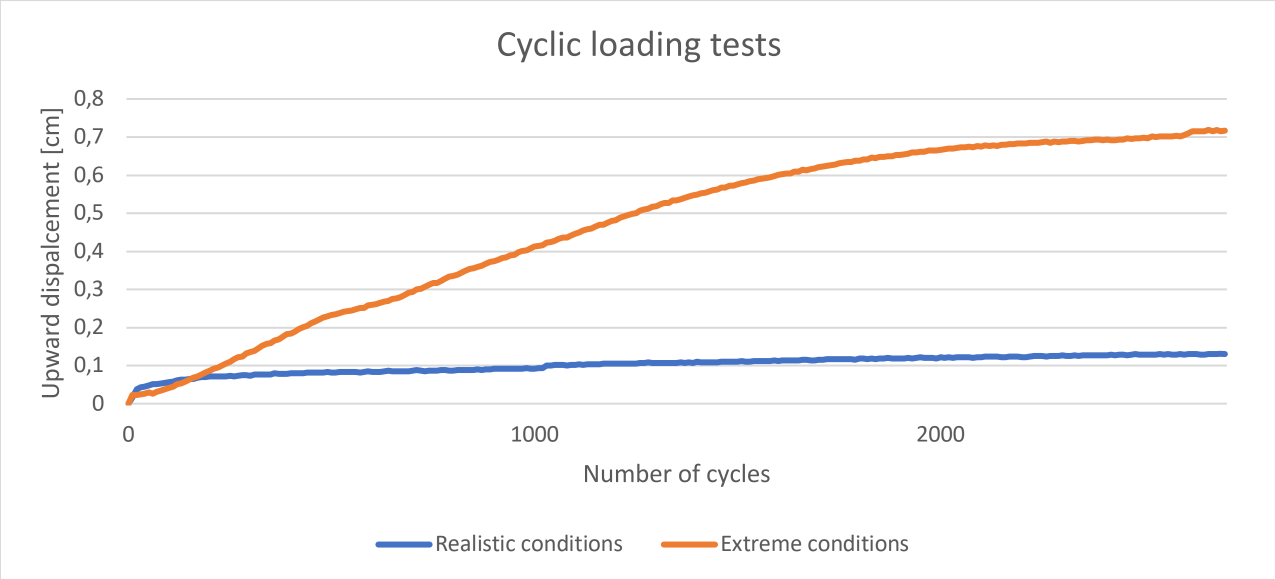

Figure 26 Displacement of RM model under cyclic loading

It was found that under 2700 stress cycles of 75N, the caisson was displaced 0,13 cm. The displacement under extreme conditions was found to be significantly higher; 0,72 cm. Both plots show similar behaviour with a slowly decreasing slope. It should be noted that the real frequency of the system is unknown at this point. However, it is expected to be multiple orders of magnitude lower than 0.2 Hz as the system is expected to inflate and deflate not more than a few times a day. Additionally, not all cycles of the bladder will be performed at full capacity. Therefore, the recorded displacement is expected to happen over a period of years.

The measured displacements scale to 13 and 72 cm respectively on the full system over a period of years. Although small (1,2 and 6,5 % of the skirt length respectively), these displacements are still undesirable. A simple solution is available to counter this problem. Once the displacement reaches a critical value, suction can be applied to "reinstall" the foundation.

7 Conclusion

An experimental study was performed to research how suction caisson behaviour is affected by a square caisson shape and by connecting multiple caissons together. These two elements are introduced by the foundation design of the Ocean Battery and the first step in assessing the technical feasibility is lab-scale testing. The performance of 5 model caissons was analysed and compared during self-weight installation, suction installation, maximum pull out and under cyclic loading. The most important observations can be summarized as follows;

The self-weight penetration behaviour of the foundation is not affected by the introduction of a square caisson shape. It does however impose a higher vulnerability to piping during suction assisted installation which is caused by the presence of sharp corners. Nonetheless, these effects can be reduced by applying a more controlled installation process and the caisson can still be installed successfully.

However, the introduction of multiple linked chambers shows worrying effects during the installation process. The self-weight penetration behaviour is very susceptible to soil bed unevenness and showed worrying results with hardly any displacement.
The required initial penetration depth was found to be 30% of the skirt length, higher than that of a single caisson. More importantly it exceeds the theoretical self-weight penetration depth of the full Ocean Battery system (20% skirt length). Based on these findings the design could not be installed successfully. However, it should be noted that it is plausible that the installation tests are affected by scaling the models and not being able to scale the sand grains.

If it is possible to install the proposed foundation, the holding capacities are not significantly influenced by the square shape and configuration. The behaviour under extraction of a square caisson was found to be almost identical to that of a cylindrical caisson. Multiple linked caissons did not cause noticeable interference when comparing the holding capacity to that of a singular caisson. Point of attention is that once reaching the critical displacement, the holding capacity of multiple linked caissons degrades at a much faster pace than that of a singular caisson. This is caused by the moment arm of the rigid structure.

Scaling the results of the row caissons to the full system resulted in a safety factor of 16 times the cyclic load imposed on the foundation by the bladder. The most representative model caisson of the Ocean Battery foundation was subjected to 2700 cycles of the proportional cyclic load of the bladder. Hardly any displacement was found. Although, imposing extreme conditions on the caisson resulted in a significantly higher displacement, the obtained values are no reason for concern, and it is concluded that the system can withstand the cyclic loading safely.

8 Discussion

Critical notes should be placed at the results obtained in this experimental study. Especially the installation process is prone for inaccuracies due to numerous factors of which scale is expected to be the most significant one. The sand could not be scaled, resulting in excessively large sand grains compared to the model caissons. It is expected that this is the reason for the large difference between the theoretical- and obtained self-weight penetration behaviour. It is unknown if the scale of the experiment affected the suction assisted installation tests as well, but it is very probable that it imposes an effect. Therefore, it is of great importance that the installation process of the foundation is further investigated to establish whether successful installation of the design is actually possible.

The flatness of the soil bed is also a contribution for inaccuracy. The bed was manually flattened before every test, but this does not ensure the exact same conditions between tests. Inevitably, some degree of unevenness exists in the soil bed that could not be measured. This unevenness can cause inaccuracies in initial penetration depths. For the row caissons (RM & PM), the displacement of individual caissons could not be measured, only the displacement of the full structure. Whether each camber of the caisson model had equal displacement could not be determined.

As the most prominent focus of the thesis was on the experimental side, the calculations put forward mainly serve as a simple comparison tool. Therefore, simplified equations were used throughout the report as the more advanced methods available were too complex for this thesis. Additionally, numerous values were extracted from literature. The developed suction for example could not be measured due to the absence of a pressure sensor and was therefore taken from (Sawicki, 2017). The same principle holds for the soil properties, determining the internal friction angle and the frictional angle between the sand and caisson was not possible. This requires very complex testing and equipment that was not available. Therefore, the properties were also taken from literature. Although the calculated values are realistic when compared to literature and showed a good accuracy with the experimental results, there is a possibility that this is just a coincidence

9 References

Ahn, J. (2015). *Finite Element Analysis of the Holding Capacity of Shallow Suction Caisson Anchors*, 33 MARINE GEORESOURCES & GEOTECHNOLOGY , 33–44

Alumni, A. E., Naqash, M. T. and Harireche, O. (2019) "A Standard Formulation for the Installation of Suction Caissons in Sand," *Journal of Ocean Engineering and Science*. doi: 10.1016/j.joes.2019.07.001.

Andersen, K. H., Jostad, H. P. and Dyvik, R. (2008) "Penetration Resistance of Offshore Skirted Foundations and Anchors in Dense Sand," *Journal of Geotechnical and Geoenvironmental Engineering*, 134(1), pp. 106–116. doi: 10.1061/(ASCE)1090-0241(2008)134:1(106).

Cheng, X. (2016). *Incremental Elastoplastic Fem for Simulating the Deformation Process of Suction Caissons Subjected to Cyclic Loads in Soft Clays*, 59 APPLIED OCEAN RESEARCH , 274–285

Harireche, O., Mehravar, M. and Alani, A. M. (2014) "Soil Conditions and Bounds to Suction during the Installation of Caisson Foundations in Sand," *Ocean Engineering*, 88, pp. 164–173. doi: 10.1016/j.oceaneng.2014.06.033.

Hung, Le Chi & Lee, Sihoon & Tran, Nghiem & Kim, Sung-Ryul. (2017). Experimental investigation of the vertical pull-out cyclic response of bucket foundations in sand. Applied Ocean Research. 10.1016/j.apor.2017.06.006.

Luke, A. M., Rauch, A. F., Olson, R. E. and Mecham, E. C. (2005) "Components of Suction Caisson Capacity Measured in Axial Pullout Tests," *Ocean Engineering*, 32(7), pp. 878–891. doi: 10.1016/j.oceaneng.2004.10.007.

Lynn, Paul A.. *Onshore and Offshore Wind Energy : An Introduction*, John Wiley & Sons, Incorporated, 2011. ProQuest Ebook Central

Malhotra, Sanjeev. (2011). Selection, Design and Construction of Offshore Wind Turbine Foundations. 10.5772/15461.

Meyerhof, G. G. (1961). The Ultimate Bearing Capacity of Foundations.
Géotechnique 1951 2:4, 301-332

Oh, K.-Y., Nam, W., Ryu, M. S., Kim, J.-Y. and Epureanu, B. I. (2018) "A Review of Foundations of Offshore Wind Energy Convertors: Current Status and Future Perspectives," *Renewable and Sustainable Energy Reviews*, 88, pp. 16–36. doi: 10.1016/j.rser.2018.02.005.

Randoh, M., Gourvernec ,S., 2009. Offshore Geotechnical Engineering. In: New York: Taylor & Francis Spon Press.

Sawicki, A., Wachowski, Ł., & Kulczykowski, M. (2016). The Pull-out Capacity of Suction Caissons in Model Investigations, Archives of Hydro-Engineering and Environmental Mechanics, 63(2-3), 157-171. doi:

Tran, M. N., Airey, D. W., & Randolph, M. F. (2005, January 1). Study of Seepage Flow And Sand Plug Loosening In Installation of Suction Caissons In Sand. International Society of Offshore and Polar Engineers.

Ukritchon B, Wongtoythong P, Keawsawasvong S. New design equation for undrained pullout capacity of suction caissons considering combined effects of caisson aspect ratio, adhesion factor at interface, and linearly increasing strength. Applied Ocean Research 2018 Jun;75:1-14.

van Dijk B. (2018. Design of suction foundations. J Zhejiang Univ Sci A 2018 Aug;19(8):579-599.

WU, Y., WANG, Z., YANG, Q. and LI, D., 2019. Theoretical studies on penetration resistance of suction caissons in clay. *Marine Georesources & Geotechnology,* **37**(5), pp. 558-567.

ZHANG, Y., LI, D. and GAO, Y., 2017. Model tests on installation and extraction of suction caissons in dense sand. *Marine Georesources & Geotechnology,* **35**(7), pp. 921-929.

Zhang, Z., Cheng, X. (2017). *Predicting the Cyclic Behaviour of Suction Caisson Foundations Using the Finite Element Method*, 12 SHIPS AND OFFSHORE STRUCTURES , 900–909

Zhou, H., Randolph, M. (2006) .*Large Deformation Analysis of Suction Caisson Installation in Clay*, 43 CANADIAN GEOTECHNICAL JOURNAL , 1344–1357